Three-dimensional measurements in the baffle region of a turbulently stirred tank
Proceedings of European Congress of Chemical Engineering (ECCE-6)
Copenhagen, 16-20 September 2007

Three-dimensional measurements in the baffle region of a turbulently stirred tank

C. Galletti, S. Pintus, E. Brunazzi

Department of Chemical Engineering, University of Pisa, Via Diotisalvi 2, I-56126 Pisa, Italy

Abstract

Three-dimensional laser Doppler Anemometry measurements of the turbulent flow field in the vicinity of the baffles in a vessel agitated with a Rushton turbine have been performed. The measurements have provided simultaneously all three components of the instantaneous velocity, and thus information on all elements of the Reynolds stress and anisotropy tensors in addition to data on flow field and turbulence levels.

Keywords: stirred vessel, baffle, Reynolds stress, turbulence, 3-D laser anemometry

1. Introduction

Traditional methods of stirred vessel design were based on overall parameters such as power requirement, pumping capacity of the impeller and circulation time within the tank. However, such global parameters do not provide any information on local phenomena which have been found to play a major role on mixing and should be considered for mixing optimisation purposes.

The smallest scales of motion govern mass and energy transfers occurring for instance in bubble break-up, coagulation, flocculation and chemical reactions. Indeed these phenomena are controlled by dissipation of turbulent kinetic energy (Paul et al., 2004). In addition turbulence stresses might play an important role for all those applications where the vessel contains particles or droplets of size comparable to the size of the turbulent eddies. This is likely to happen for instance in bioreactors where the biological entities have been observed to be turbulent stress-sensitive to varying degrees; for instance some bacteria, yeast and fungi can be relatively tolerant to high shear environments whereas other organisms require low shear rate for their viability. The effects of hydrodynamic stresses on biological particles have been discussed extensively in literature (Papagianni, 2004) and they go from their death to sub-lethal effects, e.g. modulation of their metabolism. As pointed out by Joshi et al. (1996) most of the experimental studies on the hydrodynamic response of biological

organisms have been conducted in laboratory equipments such as parallel plates or cylindrical tubes which are very different from the equipments used in practice. Therefore, it is important to assess the stress levels which are present in real stirred tanks in order to choose the most appropriate agitation rates to enhance mixing without damaging the bacterial population. Recently, Ghadge et al. (2005) have investigated the effect of flow pattern (maximum and average value of turbulent energy dissipation rate, average shear rate and average turbulent normal stress) on cellulase deactivation in stirred tank bioreactors. They found that cellulase deactivation correlates well with the average turbulent normal stress.

Unfortunately the smallest scales of the flow are difficult to be characterised experimentally, even with techniques such as laser Doppler anemometry (LDA) or particle image velocimetry (PIV). For instance only a few attempts to measure directly the dissipation of turbulent kinetic energy are reported in the open literature (Baldi et al., 2004).
Consequently, along with these techniques, the role of computational fluid dynamics (CFD) is growing. Besides, advanced CFD simulations, e.g. Large Eddy Simulation (LES), appear promising in investigating small scales of motion (Yeoh et al., 2004, Derksen, 2003, Hartmann et al., 2004a, Alcamo et al., 2005), however they still need to be assessed through comparison with experimental results.
For this purpose, experimental data have to meet very high criteria in terms of accuracy and spatial resolution, and should not be restricted to mean velocity data alone, as other quantities such as Reynolds stresses are more useful for the validation of advanced CFD approaches, e.g. LES and high order turbulence models in RANS.

It is noteworthy that investigations on stirred vessels have focused attention on the impeller region, only some studies showing data on turbulent shear stresses (for a Rushton turbine, see Derksen et al., 1999, Escudiè and Linè, 2003, Galletti et al., 2004). Conversely, the literature on other vessel regions, such as baffles in not so exhaustive, despite baffles have been confirmed to play a role in mixing which is as important as that of the agitator. Baffles promote mixing by dumping the swirling motion generated by the rotation of the impeller, and effects are substantial as, for instance, the pumping number of a Rushton turbine dramatically decreases by approximately 60% (from 0.61 to 0.25, see Brunazzi et al., 2003) when removing the baffles. In addition recent LES simulations have indicated high values of the dissipation rate of the kinetic energy in the vicinity of the baffles (Micheletti et al., 2004). However baffles may have negative effects on mixing especially for viscous fluids because they can promote the formation of dead regions upstream and downstream of them and it is important to evaluate the extent of those regions.

The present investigation has focused attention on the zones upstream and downstream of the baffles. The objective is to describe the structure of the turbulent flow field in the close vicinity of a baffle. Three-dimensional velocity measurements have been performed with a laser Doppler anemometer in a vessel stirred with a D/T = 0.33 Rushton turbine. All measurements were taken in coincidence mode so that the three instantaneous velocity components were measured simultaneously; such a 3-D configuration ensures high spatial resolution and it is the only system which can

accurately correct all errors associated with the velocity bias. Mean and turbulence levels were estimated, these latter were used to evaluate the extent of the dead regions near the baffles. All six Reynolds stresses were determined.

2. Experimental apparatus and method

Measurements were taken in a T = 290 mm cylindrical vessel made of Perspex, equipped with 4 baffles of width W = T/10 and thickness t_B = T/100 equally spaced along the vessel periphery. The vessel was filled with distilled water up to a liquid level H = T and was encased inside a trough, also filled with water, in order to minimise refraction of laser beams at the tank curve surfaces. A lid was positioned at height H, to prevent entrainment of air bubbles.
The agitation was provided by a D = T/3 standard Rushton turbine placed at tank mid-height (C = T/2). The impeller blade thickness to diameter ratio was t_b = D/100. Measurements were performed with the impeller speed N = 300 rpm (Re = 47,000).
The tank was placed on a traversing system which allowed movements along the three spatial directions with an accuracy of 0.1 mm (Figure 1).

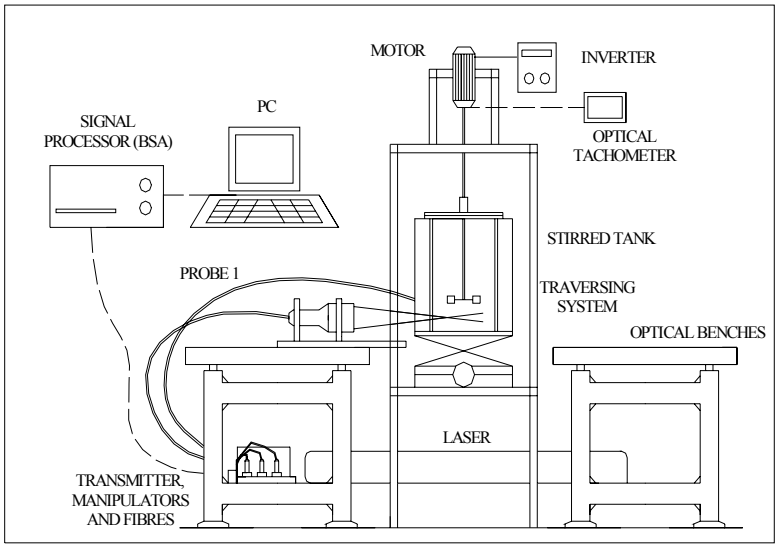

Figure 1. Experimental apparatus

A three-component Laser Doppler Anemometer (Dantec) was used to take the measurements. A 3 W Argon ion Spectra-Physics laser was split into green (λ = 514.5 nm), blue (λ = 488 nm) and purple (λ = 476.5 nm) lines. Bragg cells provided frequency shifting on all lines, and subsequently radiations were transmitted to the probes by means of optical fibres. In order to preserve and avoid damage to these fibres, the laser power was kept at 500 mW.
The system operated in orthogonal side-scatter mode (see Figure 2). The blue and green beams emerged from probe 1 and their scattered lights were collected from probe 2, which was placed at 90° to probe 1, whereas the purple beams emerged from probe 2 and their scattered light was collected from probe 1. The scattered lights were

transmitted by means of the optical fibres to the photo-multipliers and then processed by a Dantec Burst Spectrum Analyser.
The arrangement of the three laser beam pairs described above was such that the three orthogonal velocity components, i.e. u_x, u_y and u_z, could be measured: specifically u_y and u_z were measured through the blue and green beams, whereas u_x was measured through the purple beams.
The flow was seeded with silver coated hollow glass spheres with a mean diameter of 10 μm and a density of 1,400 kg/m^3.
The system operated in coincidence mode so that the three components of the velocity were taken simultaneously. The coincidence mode operation was performed by imposing that the bursts seen from the three detectors partially overlapped. In this manner only signals scattered from particles arriving at the same time in the measurement volume were validated. Special attention was paid to the setting of operating parameters such as the voltage of each of the photo-multipliers, in order to have approximately the same sensitivity for all three component measurements.

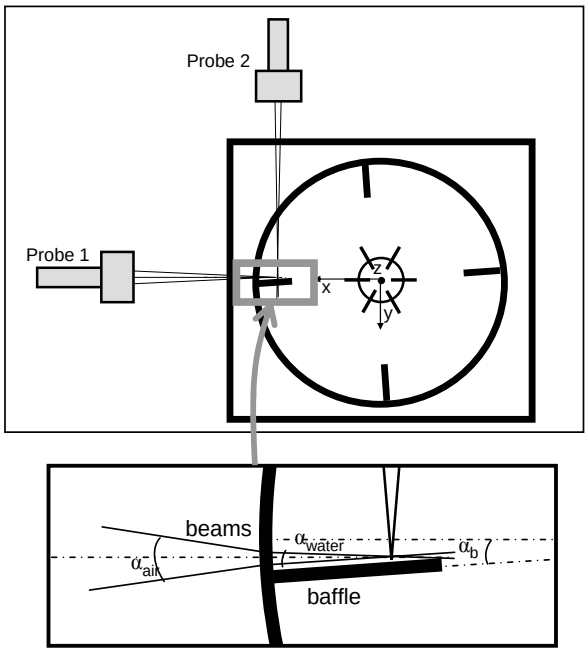

Figure 2. Spatial arrangement of mixing vessel and LDA probes

It is noteworthy that the measurement volume for this LDA setup was very small (0.0035 mm^3). This ensures an high spatial resolution, but implies a low data rate (about 5-20 Hz, partly due to the strict coincidence criterion used) as well as efforts in the system alignment (Derksen et al., 1999). At least 2,000 samples were acquired for each measurement. The data repeatability was checked by repeating each measurement a few times.
The measurement grid extended from r = 92 mm (r/T = 0.32) to r = 140 mm (r/T = 0.48) and covered an angle of 25 degrees around a baffle. Four axial planes were investigated, at z/T = 0.1, 0.3, 0.45 and 0.5T. For each plane a number of approximately 60 locations was investigated. The velocities measured in the x, y, and

z directions were transformed into axial, radial and tangential directions (u_1, u_2, u_3, respectively), according to the usual representation. This was accomplished by using a simple transformation matrix.

3. Results

3.1 Flow field

The flow field measured near the baffles is shown in Figure 3 for two different axial levels. The vectors combine radial and tangential mean velocities, whereas the colour map shows the axial velocity. The impeller was rotating clockwise.

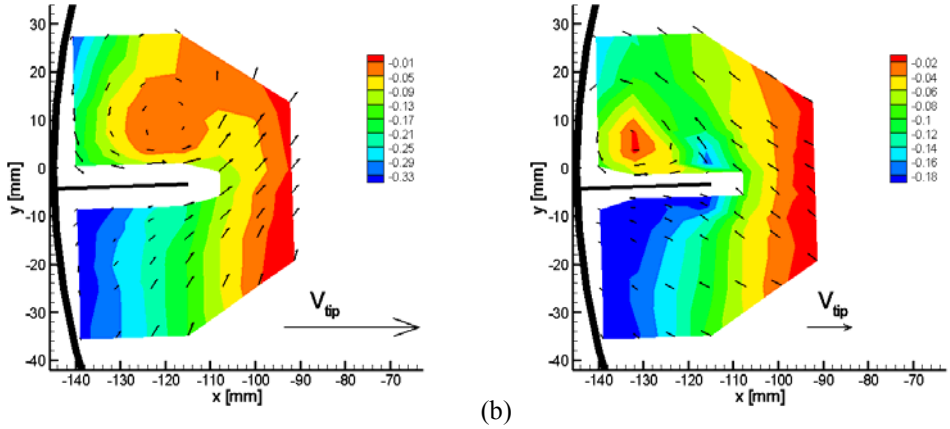

(a) (b)

Figure 3 – Flow field at (a) z/T = 0.3 and (b) z/T = 0.45. Radial and tangential mean velocities through vectors, axial mean velocity through contour plot. Impeller rotating clockwise.

At z/T = 0.3 (see Figure 3a) the vectors show that the horizontal component of the velocity near the inner edge of the baffle is inclined at about 50° with respect to the x axis, indicating higher tangential motion with respect to that at z/T = 0.1. In addition the flow field evidenced the presence of a vortex located downstream of the baffle, with the centre placed at about r =120 mm (r/T = 0.41) and a distance of d = 10 mm (d/T = 0.034) from the baffle.

As far as the axial mean velocity is concerned, high negative values were measured near the tank walls upstream of the baffle indicating that the flow was directed downwards. The maximum values were of 0.33 V_{tip}. Downstream of the baffle the flow was still directed downwards, but the mean axial velocities were much smaller. In addition it is worth noting that minimum values of the axial velocity were found in correspondence of the centre of the vortex described by vectors.

Moving up at z/T = 0.45 (see Figure 3b), the flow near the baffles changed completely features. The horizontal component of the velocity (see vectors) was directed towards the tank walls. It is noteworthy that the reference vector of Figure 3b has different length than that of Figures 3a, indicating much higher radial and tangential velocity components. The flow reached the baffle with an inclination of

40° with respect to the x axis, and then divided into two flows upstream and downstream of the baffle. The former stream is directed downwards to form the lower loop generated by a Rushton turbine impeller, whereas the latter stream exhibits lower axially velocities. A clear vortex is evident downstream of the baffles, however it appears smaller and stronger than that observed at z/T = 0.3. In addition it is positioned closer to the walls, its centre being at about r =132 mm (r/T = 0.45) and a distance of d = 5 mm (d/T = 0.017) from the baffle.

3.2 Turbulent kinetic energy and Reynolds stresses

Distribution of turbulent kinetic energy $k = \sum_{i=1}^{3} \left\langle u'_i{}^2 \right\rangle / 2$, normalised with respect to V_{tip}^2, is shown in Figure 4 for the axial plane z/T = 0.5. The results show that turbulence levels decrease moving towards the walls from $k/V_{tip}^2 = 0.08$ at r = 92 mm (corresponding to r/T = 0.31) down to $k/V_{tip}^2 = 0.04$ in the proximity of the baffle at r = 116 mm (r/T = 0.4), k/V_{tip}^2 becoming less than 0.03 near the walls both upstream and downstream of the baffle. Similar trends but with lower turbulence values were observed at z/T = 0.45. Turbulence levels were lower at the other planes, i.e. z/T = 0.1 and 0.3, k/V_{tip}^2 values being less than 0.01 in the examined grid.
It is useful reporting that in the impeller region turbulence kinetic energy up to 0.18 V_{tip}^2 were measured for the investigated impeller.

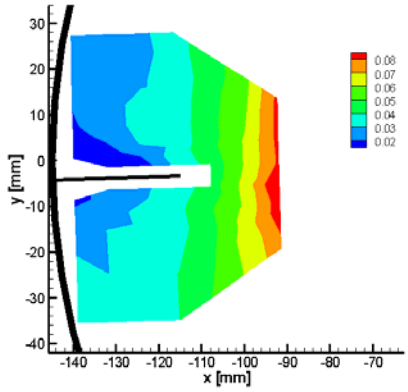

Figure 4 – Contour plot of turbulent kinetic energy, k/V_{tip}^2 at z/T = 0.5.

As mentioned previously, 3-D LDA measurements allowed determining all Reynolds stresses $R_{ij} = \left\langle u'_i \, u'_j \right\rangle$.

Ensemble-averaged distribution of the axial-radial shear stress (R_{12}) normalised with respect to V_{tip}^2 is shown, through contours in Figure 5 for the axial plane z/T = 0.45. Among the four axial planes examined, the highest R_{12} values were observed in the z/T = 0.45 plane, where R_{12} absolute values up to 0.01 V_{tip}^2 were measured for r/T between 0.3 and 0.37. Moving towards the walls, R_{12} values decreased rapidly.
Normal stresses were found to be always higher than shear stresses. Values of the axial normal stress (see Figure 6a) were higher towards the vessel axis and gradually

decreased towards the vessel walls. This may be explained by considering that walls and baffles impose a well defined axial motion to the flow, thus reducing the axial normal stresses. Somewhat higher values of axial normal stress were still present downstream of the baffles in the region where the vortex was observed.

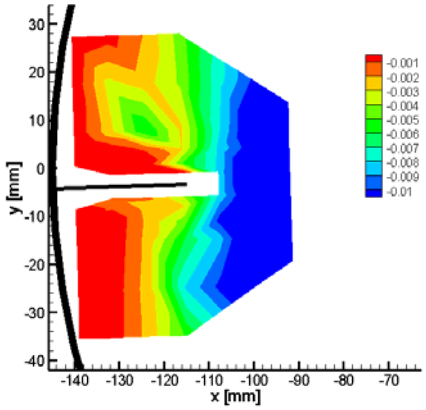

Figure 5 – Contour plot of the axial-radial Reynolds stress R_{12} / V_{tip}^2 at z/T = 0.45.

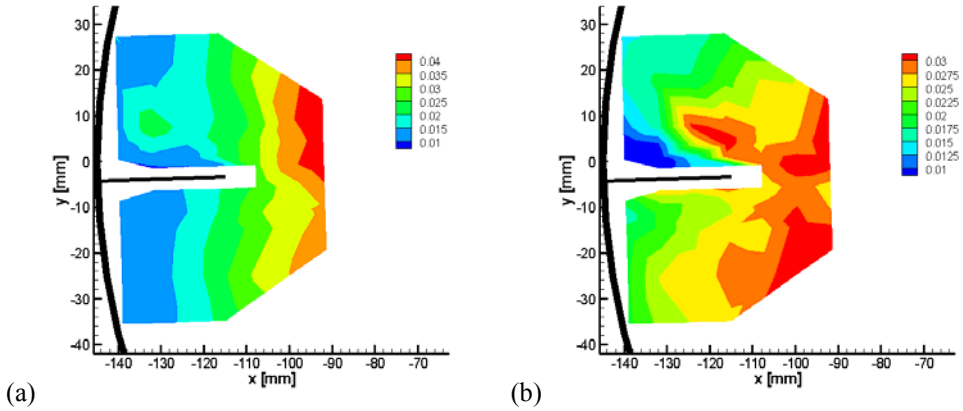

Figure 6 – Contour plot at z/T = 0.45 of (a) R_{11} and (b) R_{22}.

Radial and tangential stresses similarly decreased when moving towards the walls with maximum values of 0.3 V_{tip}^2 (see as an example R_{22} in Figure 6b).
Normal stresses in the plane at z/T = 0.5 showed maximum values about double than those described for z/T = 0.45; this is a logical consequence of the discharged stream behaviour.

3.3 Anisotropy of turbulence

Estimation of levels of anisotropy of turbulence is important to assess the correctness of using a turbulence model based on isotropy assumption, such as the popular k-ε

model. Moreover, information on levels of local anisotropy of turbulence may help the formulation of numerical models for stirred tanks.
A convenient method for the characterisation of the local anisotropy/isotropy of turbulence is provided by the analysis of the normalised Reynolds stress anisotropy tensor:

$$b_{ij} = \frac{\langle u_i u_j \rangle}{2k} - \frac{1}{3} \cdot \delta_{ij}$$

and its invariants (Lumley, 1978). b_{ij} has got real eigenvalues and the first invariant equal to zero by definition. Therefore the anisotropy tensor can be characterised by only the second (II) and the third (III) invariants. According to Lumley (1978) each point and time in a turbulent flow may be represented inside a "triangle" in the (III, -II) plane. The origin of the plane represents isotropic turbulence, therefore Derksen et al. (1999) suggested using the distance L of the point from the origin mark to characterise local anisotropy of turbulence by means of a single parameter:

$$L = \sqrt{III^2 + (-II)^2}$$

The maximum allowable L value is $L_{max} = 0.34$.

Ensemble-averaged results of L are shown in Figure 7a for the z/T = 0.5 axial plane. The colour map indicates isotropic turbulence except for a small region downstream of the baffle showing L values up to 0.035. Slightly higher values are observable at z/T = 0.45. Results are in good accordance with observations reported in earlier work (Galletti et al. 2004). Similarly at z/T = 0.3, turbulence was found to be fairly isotropic.

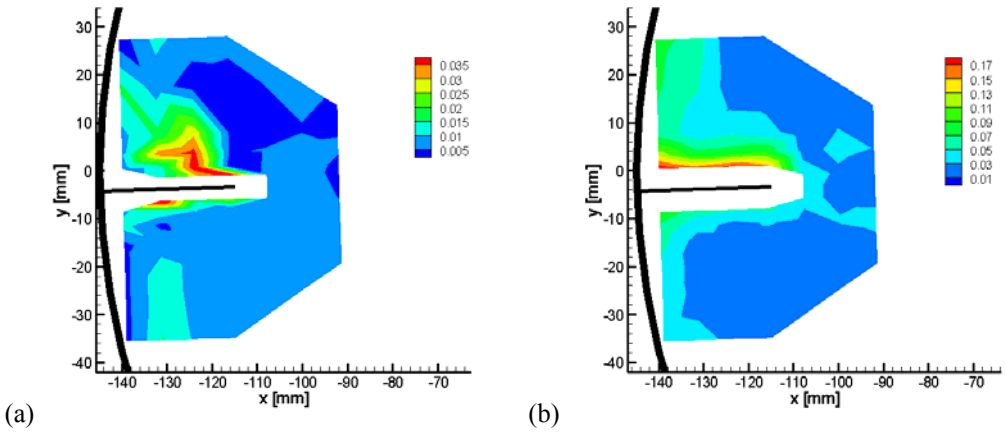

(a) (b)

Figure 7 – Contour plot of L at (a) z/T = 0.5 and (b) z/T = 0.1.

Conversely, very strong deviation from isotropy occurred in the plane at z/T = 0.1, where values of L as high as 0.17 were obtained downstream of the baffle. Results are presented in Figure 7b.

The observed L value of 0.17 is very large if compared with results presented in Galletti et al. (2004) where maxima around 0.1 were observed in the vicinity of the impeller and near the vessel bottom. Nevertheless, in the aforementioned work measurements were taken in the vertical plane midway two neighbouring baffles.
Additional results on anisotropy of turbulence across the entire vessels were provided by the LES simulations of Hartmann et al. (2004b), although they were performed with a Rushton turbine set at C/T = 0.33. The authors also showed large levels of anisotropy of turbulence near the walls and the vessel bottom. It is worth reminding that Hartmann et al. normalised the anisotropy stress tensor with respect to the kinetic turbulent energy, whereas in the present work the original definition of Lumley (1978), also used in Galletti et al. (2004), has been applied and the anisotropy stress tensor was normalised by twice the kinetic energy. For instance L = 0.17 corresponds to a value of 0.74 if calculated according to the normalisation of Hartmann et al. (2004b).

4. Conclusions

3-D LDA measurements have been taken in the vicinity of the baffles providing simultaneously all three components of the instantaneous velocity, and thus information on all elements of the Reynolds stress and anisotropy tensors in addition to data on flow field and turbulence levels.

The flow field results indicated the presence of a vortex downstream of the baffle. The centre of such a vortex was located close to the baffle and the walls around the impeller mid-height, however the centre moved towards the inner edge of the baffle when decreasing the axial plane level. In addition the vortex was smaller and stronger at the impeller mid-height, becoming weaker when moving downwards.

Data on Reynolds stresses have been provided and may help the critical evaluation of simulations that predict Reynolds stresses (i.e. LES and simulations employing high order closure models), as mean velocity data are not sufficient for comparison purposes.

Levels of anisotropy of turbulence were also determined with the Lumley's method and it was found that turbulence deviates largely from isotropy near the baffle and the bottom of the vessel. In particular levels of anisotropy of turbulence were larger than those observed near the impellers by Derksen et al. (1999) and Galletti et al. (2004). This can be worth of further attention as baffles have been proved to be responsible for up to 15% of dissipation of turbulent kinetic energy (Micheletti et al., 2004); so isotropic turbulence model may lead to significant errors in CFD predictions.

Acknowledgements

This work was financially supported by the "Ministero dell'Istruzione, dell'Università e della Ricerca Scientifica" (PRIN 2005 project).

Notation

b_{ij}	elements of the normalised anisotropy stress tensor
C	impeller off-bottom clearance, m
D	impeller diameter, m
H	liquid height, m
II	second invariant of the normalised anisotropy stress tensor
III	third invariant of the normalised anisotropy stress tensor
k	kinetic turbulent energy, $m^2 \cdot s^{-2}$
L	parameter for the estimation of the degree of anisotropy of turbulence
N	impeller rotational speed, s^{-1}
r	radial co-ordinate measured from the vessel axis, m
Re	impeller Reynolds number, $Re = \rho \cdot N \cdot D \cdot \mu^{-1}$
R_{ij}	elements of the Reynolds stress tensor, $m^2 \cdot s^{-2}$
T	tank inner diameter, m
t_b	disk and blade thickness, m
t_B	baffle thickness, m
u	instantaneous velocity, $m \cdot s^{-1}$
u’	fluctuating velocity, $m \cdot s^{-1}$
V_{tip}	impeller blade tip velocity $V_{tip} = \pi ND$, $m \cdot s^{-1}$
W	baffle width, m
x	spatial co-ordinate, m
z	axial co-ordinate measured from the vessel bottom, m
<>	temporal mean

Greek symbols

α_b	angle of the baffle with respect to x direction, degrees
θ	phase-resolved angle from the middle of reference blade, degrees
δ_{ij}	Kronecker delta
λ	laser beam wavelength, m
μ	dynamic viscosity, Pa·s
ρ	density, $kg \cdot m^{-3}$

Subscripts

1	axial
2	radial
3	tangential
x, y, z	indices indicating co-ordinate direction
i,j	indices
max	maximum

References

Alcamo, R., Micale, G., Brucato, A., Ciofalo, M. (2005). *Chemical Engineering Science* **60**, 2303.

Baldi, S., Ducci, A., Yianneskis, M. (2004). *Chemical Engineering and Technology* **27**, 275.

Brunazzi, E., Galletti, C., Paglianti, A., Pintus, S. *AIDIC Conference Series* **6**. AIDIC Milano-Italy, 67 (2003).

Derksen, J.J. (2003). *American Institute of Chemical Engineers Journal* **49**, 2700.

Derksen, J.J., Doelman, M.S., Van den Akker, H.E.A. (1999). *Experiments in Fluids* **27**, 522.

Escudiè, R., Linè, A. (2003). *American Institute of Chemical Engineers Journal* **49**, 585.

Galletti, C., Brunazzi, E., Pintus, S., Paglianti, A., Yianneskis, M. (2004). *Transactions IChemE, Chemical Engineering Research and Design* **82**, 1214.

Ghadge, R.S., Patwardhan, A.W., Sawant, S.B., Joshi, J.B. (2005). *Chemical Engineering Science* **60**, 1067.

Hartmann, H., Derksen, J.J., Van den Akker, H.E.A. (2004a). *American Institute of Chemical Engineers Journal* **50**, 2383.

Hartmann, H., Derksen, J.J., Montavon, C., Pearson, J., Hamill, I.S., Van den Akker, H.E.A. (2004b). *Chemical Engineering Science* **59**, 2419.

Joshi, J.B., Elias, C.B., and Patole, M.S. (1996). *Chemical Engineering Journal* **62**, 121.

Lumley, J. (1978). *Advanced Applied Mechanics* **26**, 123.

Micheletti, M., Baldi, S., Yeoh, S.L., Ducci, A., Papadakis, G., Lee, K.C., Yianneskis, M. (2004). *Transactions IChemE, Chemical Engineering Research and Design* **82**, 1188.

Papagianni, M. (2004). *Biotechnology Advances* **22**, 189.

Paul, E., Atiemo-Obeng, V.A., Kresta, S.M. *Handbook of Industrial Mixing. Science and Practice*, John Wiley & Sons, Inc. (2004).

Yeoh, S.L., Papadakis, G., Lee, K.C., Yianneskis, M. (2004). *Chemical Engineering Technology* **27**, 257.